The effects of separating inferior alveolar neurovascular bundles on osteogenesis of tissue-engineered bone and vascularization

Lin Feng[#], Lingling E[#], Hongchen Liu

Aim. To evaluate the effects of autologous blood vessels and nerves on vascularization.
Methods. A dog model of tissue-engineered bone vascularization was established by constructing inferior alveolar neurovascular bundles through the mandibular canal. Sixteen 12-month-old healthy beagles were randomly divided into two groups (n=8). Group A retained inferior alveolar neurovascular bundles, and Group B retained inferior alveolar nerves. Bone marrow mesenchymal stem cells were injected into β-tricalcium phosphate to prepare internal tissue-engineered bone scaffold. A personalized titanium mesh was then prepared by rapid prototyping and fixed by external titanium scaffold. Two dogs in each group were sacrificed on the 30th, 45th, 60th and 90th postoperative days respectively. The bone was visually examined, scanned by CT, and subjected to HE staining, immunohistochemical staining, vascular casting and PCR to detect the changes in osteogenesis and vascularization.
Results. The two groups had similar outcomes in regard to osteogenesis and vascularization ($P>0.05$): both showed remarkable regenerative capacities.
Conclusions. The model of tissue-engineered bone vascularization is potentially applicable in clinical practice to allow satisfactory osteogenesis and vascularization.

Key words: inferior alveolar neurovascular bundle, osteogenesis, tissue-engineered bone, vascularization

Received: February 6, 2014; Accepted: September 16, 2014; Available online: October 29, 2014
http://dx.doi.org/10.5507/bp.2014.050

Department of Stomatology, Chinese PLA General Hospital, Beijing 100853, P. R. China
[#]The authors contributed equally to this work
Corresponding author: Hongchen Liu, e-mail: liuhongchen3011@gmail.com

INTRODUCTION

Speed and quality are equally important in studies regarding tissue-engineered bones. Therefore, it is imperative to repair large bone defects in clinical practice with satisfactory postoperative appearance and functional recovery[1].

Since the revascularization of large tissue-engineered bones, which depends on the ingrowth of peripheral blood vessels, is time-consuming, material-complexed osteoblasts may have died before the reestablishment of normal blood circulation. Hence, blood supply should be restored as soon as possible to retain the osteogenic activity of complex materials[2]. Sahota et al.[3] mainly ascribed the failure of tissue-engineered implants to slow vascularization. Besides, it is impossible to provide favorable conditions, such as constant temperature, pH, and continuous supply of nutrients and oxygen, for the growth of seed cells inside large scaffold materials. Accordingly, tissue-engineered materials can only be thin and small before building neurovascular tissue-engineered bones by combining effective vascular bundles with sensory nerve bundles. Under normal conditions, only the cells 20~200 μm away from the capillaries *in vivo* can be nourished through diffusion[4], whereas those *in vitro* (100~200 μm) cannot be sufficiently supplied with nutrients and oxygen[5]. In other words, the nutrients and oxygen content decrease gradiently with enlarging scaffold material. Under the same growth conditions, the seed cells inoculated in scaffold materials continuously reproduce and differentiate inward, leading to the death of central cells owing to hypoxia[6].

Given that a functional vascular network is dispensable in bone healing, the vascularization of scaffold materials predominantly controls the construction of high-quality tissue-engineered bones[7].

In the field of tissue engineering, standardized animal models bridge experimental studies and clinical use as the scientific basis[8]. The capacity of a tissue-engineered bone candidate's regenerating bone defects can be evaluated by being implanted in different types of animal models. Commonly, large (e.g. sheep, goat, dog and pig) and small (e.g. rat, mouse and rabbit) animal models are used[9].

In this study, a dog model of tissue-engineered bone vascularization was established by constructing inferior alveolar neurovascular bundles through the mandibular canal.

MATERIALS AND METHODS

Experimental animals

Sixteen 12-month-old healthy beagles were provided by the Laboratory Animal Center, Chinese PLA General Hospital without gender limitation. All experiments were in compliance with protocols and policies approved by the Animal Care and Use Committee of Chinese PLA

General Hospital. They were randomly divided into two groups (n=8), i.e. Group A that retained inferior alveolar neurovascular bundles, and Group B that retained inferior alveolar nerves.

In vitro preparation of tissue-engineered bones

Each beagle was anesthetized by being intramuscularly injected with a mixture of sumianxin, ketamine and atropine. Red bone marrow was collected from bilateral iliac bones (5 mL in total, containing bone marrow mesenchymal stem cells). Then the cells were prepared into osteoblasts (10^6/mL) after primary culture, subculture and induced differentiation, and were inoculated in β-tricalcium phosphate (β-TCP) to prepare the tissue-engineered bones.

Preparation of internal and external tissue-engineered bone scaffolds

The mandibles were scanned by high-resolution spiral CT, based on which a defect model was designed and sent to a factory via email for rapid prototyping. Then personalized titanium mesh, external titanium scaffold and β-TCP internal tissue-engineered bone scaffold were prepared.

Mandible reconstruction surgery

Unilateral teeth were extracted after anesthesia according to a previously designed method. Mucoperiosteum was separated through an incision 15 mm below the extraoral mandibular edge, and 15 mm above the lower edge of the mandible was incised by a piezotome. Square defect areas (lengths: about 20-33 mm) were prepared along the premolars and molars on one side of the mandible while protecting the inferior alveolar neurovascular bundle. After hemostasis, the inferior alveolar artery in Group A was truncated (1 cm long), and the inferior alveolar nerve in Group B was truncated (1 cm long). Subsequently, the truncated residues and the inferior alveolar neurovascular bundle membrane were sutured, and hemorrhaging was stopped. External and internal scaffolds were installed, and soft tissues were sutured and embedded before hemostasis. The surgical wounds were rinsed by normal saline, sutured layeredly, and bandaged. The beagles were then intramuscularly injected with 400000 U penicillin daily after surgery for three consecutive days (qd). Finally, the two groups were CT-scanned on the 60th and 90th postoperative days to observe the histological changes (Fig. 1).

Real-time quantitative PCR and RT-PCR

Real-time PCR and RT-PCR were used to quantify the levels of transcript-encoding factors in the two groups. To isolate total RNA for reverse transcription-polymerase chain reaction (RT-PCR), the BMSCs were seeded on β-TCP at 1×10^5 cells/cm^2 graft for 24 h to allow attachment in ordinary media. The cells were starved using a serum-free medium containing 2% bovine serum albumin, 100 U/Ml penicillin, and 100 mg/L streptomycin for 24 h. After 14 days of culture, the BMSCs were crushed in lysis buffer (Roche) with an RNase-free piston (Pellet), vortexed, and spun. The clear cell lysate was transferred to QiaShredder (Qiagen, Inc.) columns for RNA purification. RNase-Free DNase (Roche) was used to eliminate DNA contamination of RNA samples. Purified RNA was dissolved in RNase-free water and its concentration was assessed by reading at 260 nm. RNA quality was checked on a 2% agarose gel with 1 mg/mL ethidium bromide. Samples were stored at 808 °C until use. Complementary DNA (cDNA) was synthesized from 2 mg of total RNA with the first-strand cDNA synthesis kit for RT-PCR (AMV; Roche). Eight microliters of cDNA mixture diluted 1:20 in water was subjected to real-time PCR using SYBR Green I dye (Lightcycler faststart DNA master SYBR green I; Roche). Reactions were performed in 20 mL PCR mixture containing 4 μL 5× Master Mix (dNTP mixture with dUTP instead of dTTP, $MgCl_2$, SYBR Green I dye, Taq DNA Polymerase, and reaction buffer) and 2 mL of 10 mM primers. β-Actin real-time PCR was run as a control to monitor RNA integrity and to be used for nor-

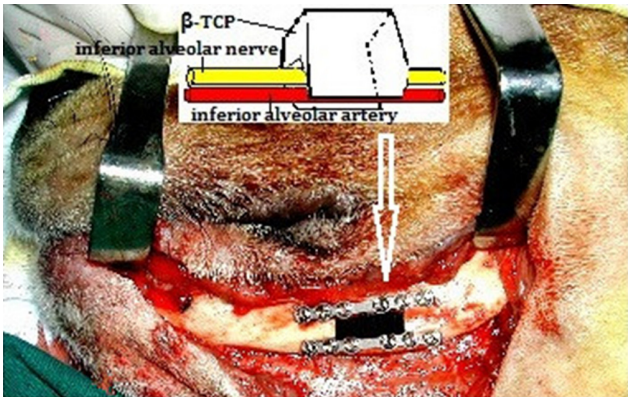

Fig. 1. Mandible reconstruction surgery outcomes: surgical installation of external and internal scaffolds.

Table 1. Primers used for real-time quantitative PCR and RT-PCR.

Gene	Primer sequence	Product size (bp)
ALP	F: 5'-TCC CAC GTT TTC ACG TTT-3'	140
	R: 5'-GAG ACG TTC TCC CGT TCA C-3'	
OCN	F: 5'-TGA GGA CCC TCT CTC TGC TC-3'	150
	R: 5'-AGG TAG CGC CGG AGT CTA TT-3'	
COL	F: 5'-CTA CAG CAC GCT TGT GGA TG-3'	192
	R: 5'-ATT GGG ATG GAG GGA GTT TA-3'	
β-Actin	F: 5'-CCC ATC TAT GAG GGT TAC CC-3'	150
	R: 5'-TTT AAT GTC ACG CAC GAT TTC-3'	

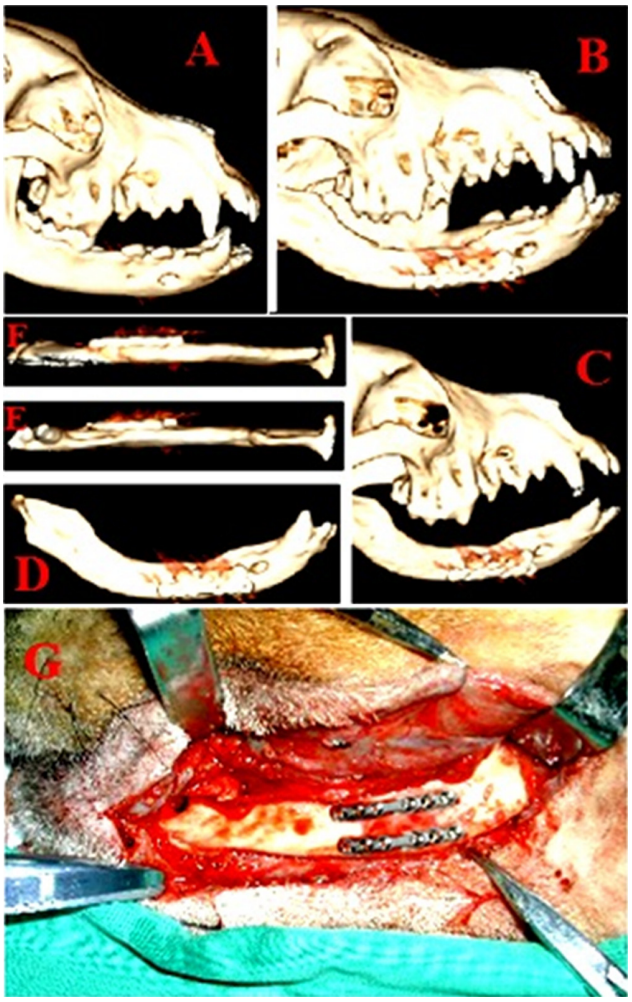

Fig. 2. A: CT scanning image of No. 1 beagle in Group A before surgery; B: scanning image of No. 2 beagle in Group A on the 90th postoperative day; C: scanning image of No. 2 beagle in Group B on the 90th postoperative day; D-F: local scanning images of No. 2 beagle in Group A on the 90th postoperative day; G: naked-eye observation of No. 3 beagle in Group A on the 90th postoperative day.

malization. Specificity of each primer pair was confirmed by melting curve analysis (Table 1).

RESULTS

General information of animals

On the 1st postoperative day, all beagles were fatigued and not interested in eating or moving. The limbs receiving surgery were obviously lame, with normal peripheral skin temperature and blood circulation. They were more inclined to eat and move actively 3 days later. One dog that succumbed to local infection was treated by replacing the scaffold material. All dogs were free of mandibular fracture.

Preliminary observation

Bony callus increased till the 60th day and gradually connected as the bone defect area, and the material was basically ossified on the 90th day.

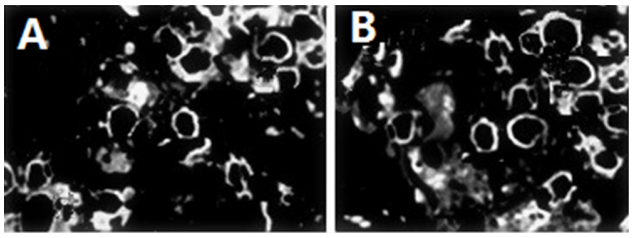

Fig. 3. CD31 immunohistochemical staining results of Group A (A) and Group B (B) on the 90th day. Bar, 50 μm.

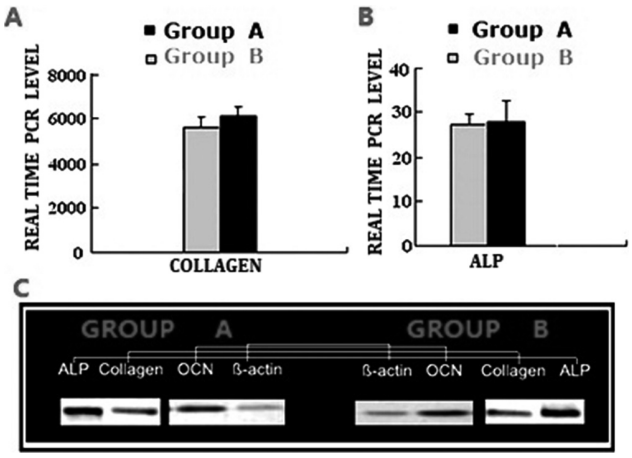

Fig. 4. Real-time quantitative PCR and RT-PCR results.

CT observation

CT scanning on the 30th postoperative day disclosed that the bone defect was healed by being connected with the 3D reconstructed material, accompanied by increased bony calli and material absorption. On the 90th day, there was density increase in the bone defect area, while the absorption was not evident. Both groups experienced significantly enhanced osteogenesis on the 90th day compared with those on the 30th day ($P<0.05$). This aside, similar bones formed in the two groups (Fig. 2).

Histological and morphometric analyses

Immunohistochemical staining showed that numerous vascular structures appeared on the 90th day, and the two groups were of similar amounts of neovascular tissues (Fig. 3).

Vascular casting results - vascularization after implantation.

The implants were extracted on the 30th, 45th, 60th and 90th postoperative days, and prepared into sections that were subjected to CD31 staining to observe the number of new blood vessels (Table 2).

The number of new blood vessels in Group A was similar to that of Group B. Microvessels were clearly visible, and blood vessels reticulated along Haversian and Volkmann's canals. Meanwhile, nutrient vessels grew into endostea and periostea. There were Haversian canals in the middle as well as in internal and external lamel-

Table 2. Numbers of microvessels at each time point.

	n	30th day	45th day	60th day	90th day
Group A	8	5.76±1.03	20.23±3.79	34.75±8.23	47.89±9.84
Group B	8	5.20±0.67	19.87±2.27	33.22±6.76	47.30±7.64
t		2.635	1.727	2.271	1.582
P		0.9782	0.9836	0.9442	0.9628

lae, with blood vessels reticulating along Haversian and Volkmann's canals.

The real-time quantitative PCR and RT-PCR results are presented in Fig. 4. The similar ALP activity, OCN content, and mineral formation of BMSCs indicated that Group A and B provided the same environment for the osteogenic differentiation of BMSCs.

DISCUSSION

Significance of constructing model of tissue-engineered bone vascularization

Constructing tissue-engineered bone is the optimum strategy for repairing large bone defects. Since tissue engineering is intrinsically bionic, it is necessary to establish a vascular network that dominates in the formation of bone tissues and the healing of bone fracture for *in vitro* construction of tissue-engineered bone. Schmid et al.[10] repaired a rabbit model of skull defects with resorbable polymer films and fibers. In the 4th postoperative week, the formations of new bones and blood vessels were related temporally and spatially. Currently, tissue-engineered bones are mainly vascularized by using materials, seed cells, cytokines, as well as microsurgical implantations of fascia-wrapping materials and vascular bundles with blood supply[11].

Stein et al.[12] found that the ingrowth of microvessels in the regions receiving tissue-engineered bone, i.e. vascularization, could carry considerable osteoblast precursor cells, related signaling molecules, nutrients, and other cells participating in bone formation and repair in the target local environment, and thereafter could eliminate the products of vigorous metabolism. Nomi et al.[13] introduced protocols concerning complexation of engineered tissues with vascular factors, and vascularization pretreatment before implanting endothelial cells and matrix materials. Pei[14] emphasized the importance of tissue-engineered bone vascularization, advocated the reconstruction of blood circulation with different methods, as well as evaluated the significances of microsurgical vascular bundle implantation, fascial flap wrapped surgery and in situ vessel preconstruction. Hokugo et al.[15] conducted a heterotopic ossification assay to wrap saphenous vascular bundles with bioabsorbable membrane that was complexed with autogenous cancellous bone particles.

Numerous nerve fibers are distributed in bone tissues, especially in the periosteum[16]. Besides, small myelinated and unmyelinated fibers are distributed in bones with nourishing blood vessels. Konttinen et al.[17] found that there were abundant sensory and autonomic nerve fibers in normal bone tissues. Peptidergic nerve fibers that contained various neuropeptides were distributed depending on the states of bones (e.g. normal bone remodeling, fracture healing, bone connection). Moreover, the nervous system predominantly controls the formation, development, regeneration and functions of other systems. Similarly, it is indispensable in the formation, repair and reconstruction of bones. Peptidergic nerve fibers are dominant in bone tissues, mainly including calcitonin gene-related peptide (CGRP), neuropeptide Y (NPY), substance P (SP) and vasoactive intestinal peptide (VIP), of which SP and CGRP peptidergic nerves originate from sensory nerves while VIP and NPY ones stem from autonomic nerves. It is well-established that the effects of the nervous system on bone tissues are mediated by nerve growth factor (NGF) and various neuropeptides. Eppley et al.[18] treated rabbit mandibular nerve injury by NGF, and they accidentally observed that the osteogenesis surrounding axons was enhanced after being stimulated. Zhang et al.[19] constructed tissue-engineered bone by implanting nerves and verified that sensory nerves were able to remarkably promote bone formation with a *in vivo* animal model. Hence, vascularization and neuralization are equivalently important for tissue-engineered bones.

Selection and analysis of animal model

Beagles are model animals suitable for repeated experiments due to moderate body form, mild temper and easy feeding. Jin reported that the mandibular alveolar artery originated from the maxillary artery concomitant with the inferior alveolar nerve and nourished inferior teeth by its branches[20]. Li et al. reported that in the mandibular canal, inferior alveolar nerve and the concomitant blood vessels were wrapped into a neurovascular bundle by a layer of capsule. Blood vessels were continuously located at above nerves, with small branches wrapping them[21]. Yin et al. reported that the mandibular alveolar artery entered the mandible through the mandibular foramen and passed through the mandibular canal. Its branches nourished the body of the mandible and the ascending branch below the mandibular foramen[22].

Notably, inferior alveolar neurovascular bundles across the bone are easily separable in clinical practice, which is rare in human anatomy. Meanwhile, the bundles mainly provide blood for the mandible and regulate the sensory nerves. In addition, the mandibular periosteal vascular network also functions. They are both conducive to the vascularization of tissue-engineered bones. The findings herein provide preliminary evidence for relevant studies.

However, the feasibility of the animal model needs further verification by adding more control groups, establishing larger defects (>30 mm), and carrying out neuralization assays.

The model established here was successful as we expected, as evidenced by the CT scanning and histological results. Therefore, the beagle model of tissue-engineered bone vascularization was eligible because of high availability and successful rate as well as facile preparation process. Particularly, inferior alveolar neurovascular bundle is, as an autologous tissue, convenient for unraveling the mystery of human body.

CONCLUSION

In summary, the model in this study integrated blood supply in the construction of tissue-engineered bone, which offers an effective paradigm to investigate *in vivo* bone microenvironment, relationships between vascularization and neuralization factors, and dose-effect relationships for osteogenesis.

Acknowledgement: This paper was founded by "China postdoctoral science foundation", grant No. 2014M552645.
Author contributions: LF, LR: data collection, data analysis and manuscript revision; HL: study design and manuscript drafting.
Conflict of interest statement: None declared.

REFERENCES

1. Orban JM, Marra KG, Hollinger JO. Composition options for tissue-engineered bone. Tissue Eng 2002;8:529-39.
2. Jin D, Pei GX, Chen B, Qin Y. Angiogenesis and neuralization study of bone tissue engineering. Modern Rehabil 2001;8:18-9.
3. Sahota PS, Bunr JL, Brown NJ, MacNeil S. Approaches to improve angiogenesis in tissue-engineered Skin. Wound Repair Regen 2004;12:635-42.
4. Muschler GF, Nakamoto C, Griffith LG. Engineering principles of clinical cell-based tissue engineering. J Bone Joint Surg Am 2004;86-A:1541-58.
5. McClelland RE, Coger RN. Use of micropathways to improve oxygen transport in a hepatic system. J Biomech Eng 2000;122:268-73.
6. Volkmer E, Drosse I, Otto S, Stangelmayer A, Stengele M, Kallukalam BC, Mutschler W, Schieker M. Hypoxia in Static and Dynamic 3D Culture Systems for Tissue Engineering of Bone. Tissue Eng Part A 2008;14:1331-40.
7. Will J, Melcher R, Treul C, Travitzky N, Kneser U, Polykandriotis E, Horch R, Greil P. Porous ceramic bone scaffolds for vascularized bone tissue regeneration. J Mater Sci Mater Med 2008;19:2781-90.
8. Cancedda R, Giannoni P, Mastrogiacomo M. A tissue engineering approach to bone repair in large animal models and in clinical practice. Biomaterials 2007;28:4240-50.
9. Drosse I, Volkmer E, Capanna R, De Biase P, Mutschler W, Schieker M. Tissue engineering for bone defect healing: An update on a multi-component approach. Injury 2008;39 Suppl 2:S9-S20.
10. Schmid J, Wallkamm B, Hämmerle CH, Gogolewski S, Lang NP. The significance of angiogenesis in guided bone regeneration: a case report of a rabbit experiment. Clin Oral Implants Res 1997;8:244-8.
11. Wu YC. [Development of vascularization of tissue engineering bone]. Intern J Biomed Eng 2003;26:125-8.
12. Stein H, Perren SM, Cordey J, Kenwright J, Mosheiff R, Francis MJ. The muscle bed-a crucial factor for fracture healing: a Physiological concept. Orthopedics 2002;25:1379-83.
13. Nomi M, Atala A, Coppi PD, Soker S. Principals of neovascularization of tissue-engineering. Mol Aspects Med 2002;23:463-83.
14. Pei GX. The status quo and tendency of bone tissue engineering research. Med J Chin PLA 2002;27:471-4.
15. Hokugo A, Kubo Y, Takahashi Y, Fukuda A, Horiuchi K, Mushimoto K, Morita S, Tabata Y. Prefabrication of vascularized bone graft using guided bone regeneration. Tissue Eng 2004;10:978-86.
16. Nör JE, Peters MC, Christensen JB, Sutorik MM, Linn S, Khan MK, Addison CL, Mooney DJ, Polverini PJ. Engineering and characterization of functional human microvessels in immunodeficient mice. Lab Invest 2001;81:453-63.
17. Konttinen Y, Imai S, Suda A. Neuropeptides and the puzzle of bone remodeling. State of the art. Acta Orthop Scand 2006;67:632-9.
18. Eppley BL, Snyders RV, Winkelmann TM, Roufa DG. Efficacy of nerve growth factor in regeneration of the mandibular nerve: a preliminary report. J Oral Maxillofac Surg 1991;49:61-8.
19. Zhang YP, Cui JX, Pei GX, Wang YG, Jin D, Qin Y, Chen B, Wei KH. [A primary study on reconstruction of neuralization of tissue engineered bone]. Chin J Orthop Trauma 2005;7:60-5.
20. Jin SQ. Practical Anatomy for Surgeons. Xi'an: Shaanxi Science and Technology Press; 2002. p. 194-5.
21. Li NY, Zhao BD, Yang XC, Tan CX, Gong DL. Intramandibular course and anatomic structure of the inferior alveolar nerve canal. Chin J Stomatol 2001;36:446-7.
22. Yin XM, Dai JX, Wang XH, Xu DC, Zhong SZ. Observation of Blood Supplies System to Mandible in Transparent Specimen. Shanghai J Stomatol 2003;12:266-8.